# The Cell Penetrating Peptides pVEC and W2-pVEC Induce Transformation of Gel Phase Domains in Phospholipid Bilayers without Affecting Their Integrity†

Michael E. Herbig,‡ Fabiano Assi,§,|| Marcus Textor,§ and Hans P. Merkle*,‡

*Drug Formulation & Delivery Group, Department of Chemistry and Applied BioSciences, Swiss Federal Institute of Technology Zurich (ETH Zurich), Wolfgang-Pauli-Strasse 10, CH-8093 Zurich, Switzerland, and Laboratory for Surface Science and Technology, Department of Materials, Swiss Federal Institute of Technology Zurich (ETH Zurich), Wolfgang-Pauli-Strasse 10, CH-8093 Zürich, Switzerland*

*Received May 18, 2005; Revised Manuscript Received December 20, 2005*

ABSTRACT: The cell penetrating peptide (CPP) pVEC has been shown to translocate efficiently the plasma membrane of different mammalian cell lines by a receptor-independent mechanism without exhibiting cellular toxicity. This ability renders CPPs of broad interest in cell biology, biotechnology, and drug delivery. To gain insight into the interaction of CPPs with biomembranes, we studied the interaction of pVEC and W2-pVEC, an Ile → Trp modification of the former, with phase-separated supported phospholipid bilayers (SPB) by atomic force microscopy (AFM). W2-pVEC induced a transformation of dipalmitoyl phosphatidylcholine (DPPC) domains from a gel phase state via an intermediate state with branched structures into essentially flat bilayers. With pVEC the transformation followed a similar pathway but was slower. Employing fluorescence polarization, we revealed the capability of the investigated peptides to increase the fluidity of DPPC domains as the underlying mechanism of transformation. Due to their tighter packing, sphingomyelin (SM) domains were not transformed. By combination, AFM observations, dynamic light scattering studies, and liposome leakage experiments indicated that bilayer integrity was not compromised by the peptides. Transformation of gel phase domains in SPB by CPPs represents a novel aspect in the discussion on uptake mechanisms of CPPs.

Difficult transportation through the cell membrane is a notorious hallmark for the cellular delivery of many large and hydrophilic therapeutics. To aid in this process, several classes and/or prototypes of cell-penetrating peptides (CPPs[1]) have been proposed during the past decade (*1*−*3*). Mostly, CPPs are short peptides of about 10 to 30 amino acids, many of them of strongly cationic nature, which may be covalently conjugated to the cargo of interest. Moreover, many CPPs form noncovalent electrostatic complexes with nucleic acid cargoes such as DNA or oligonucleotides (*4*, *5*). By hydrophobic interactions, CPPs even have the capacity to form noncovalent complexes with large proteins carrying hydrophobic binding sites (*6*) The ability of the CPPs to translocate a therapeutic cargo, particularly peptide, protein, and nucleic acid biopharmaceuticals, across cellular membranes renders them of broad interest in cell biology, biotechnology, and drug delivery. In fact, CPPs have been used as vectors for the cytoplasmic and nuclear delivery of hydrophilic biomolecules and drugs (*7*−*9*).

There are currently two principal avenues to analyze the principles of CPP function. Cellular studies come first, using proliferating or confluent cell models with the aim, e.g., to identify the capacities of distinct CPPs for translocation, their pertinent pathways and routes for cellular traffic, and the thereby involved mechanisms. A second branch in current CPP research is the study of the interactions of CPPs with lipid bilayer and monolayer models of various lipid compositions. To this end, a large body of different methodologies is available, including liposome leakage, liposome partitioning, the study of microviscosity, electrical resistance, interaction with giant vesicles, and NMR, CD, or IR based spectroscopy on the interactions of CPPs with lipid mono- and bilayers. Although rather distant from the actual cell biology of CPP translocation, the flavor of such methodologies lies in the clear definition of the experimental setup, sometimes at the expense of biological relevance. Nevertheless, when considered in conjunction with the cell biology of translocation, the physicochemical analysis of CPP/lipid membrane interactions remains an indispensable tool. For the CPPs investigated in this study translocation studies in

† This work was supported by the Commission of the European Union (EU project on Quality of Life and Management of Living Resources, Project No. QLK2-CT-2001-01451).

* To whom correspondence should be addressed. Tel: +41-44-6337310. Fax: +41-44-6337314. E-mail: hmerkle@pharma.ethz.ch.

‡ Drug Formulation & Delivery Group, Department of Chemistry and Applied BioSciences.

§ Laboratory for Surface Science and Technology, Department of Materials.

|| Present address: Baverstam Associates, Carouge-Geneva, Switzerland.

[1] Abbreviations: AFM, atomic force microscopy; CPP, cell penetrating peptide; $\Delta G_{wif}$, whole residue free energy of transfer from water to POPC interface; $\Delta G_{oct}$, whole residue free energy of transfer from water to octanol; DLS, dynamic light scattering; DPC, dodecyl phosphocholine; DPH, 1,6-diphenyl-1,3,5-hexatriene; DOPC, 1,2-dioleoyl-phosphatidylcholine; DPPC, 1,2-dipalmitoyl-phosphatidylcholine; EDTA, ethylenediamine tetraacetic acid; HEPES, 4-(2-hydroxyethyl)-1-piperazineethanesulfonic acid; LUV, large unilamellar vesicle; MLV, multilamellar vesicle; PBS, phosphate buffered saline; POPC, 1-palmitoyl-2-oleoyl-phosphatidylcholine; pVEC, vascular endothelial cadherin-derived CPP; SPB, supported phospholipid bilayer.

10.1021/bi050923c CCC: $33.50 
Published on Web 02/25/2006

cell culture models have been previously reported (*10*−*12*). Independently of their function as CPP, we propose them to induce a yet unknown transformation mechanism in phospholipid bilayers.

An initial event in CPP translocation is believed to be the interaction of a CPP, or its covalent conjugate or complex thereof, with the cell membrane, possibly leading to an enrichment in or perturbation of the phospholipid bilayer, which may subsequently trigger endocytic uptake (*13*−*18*). During the past decade, atomic force microscopy (AFM) of supported phospholipid bilayers (SPBs) has become a tool in the analysis of membrane models, particularly for the study of the interactions of drugs, peptides, and proteins with phospholipid bilayers (*19*). The major assets of AFM are (i) the capacity to probe the surface structure of SPBs in real time and under conditions close to physiological, (ii) the flexibility to modify SPB composition and structure, and (iii) the opportunity to measure physical properties directly and at very high spatial resolution. In aqueous buffers structure topologies may be acquired with a lateral resolution of 0.5−1 nm and a vertical resolution of 0.1−0.2 nm (*20*).

So far, mainly distribution and aggregation phenomena and effects of physiological proteins on SPB membrane restructuring have been characterized by AFM (*21*−*25*). Further, successful visualizations were reported for the formation of striated domains in DPPC bilayers induced by transmembrane peptides (*26*, *27*), and the dissolution process of DOPC bilayers induced by the pore-forming peptide melittin (*28*). Despite the great potential of AFM to contribute to a better understanding of CPP action on lipid membranes, so far only a single AFM study featuring CPP effects on SPBs has been published. In that study, a human calcitonin derived CPP, hCT(9-32), alone or coupled to a protein cargo, has been studied to aggregate in the DOPC fluid phase of DOPC/DPPC phase-separated SPBs in the absence of cholesterol, and in the DPPC liquid ordered phase, when cholesterol was present (*29*). Aggregation was previously considered to trigger the endocytosis of human calcitonin and a CPP derivative thereof (*30*).

In the present study, we investigated the effects of two CPPs, pVEC and W2-pVEC, a single point modification, replacing Leu in position 2 by Trp, on DOPC/DPPC phase-separated SPBs. pVEC, a peptide derived from the murine vascular endothelium cadherin (VE-cadherin), contains 18 amino acids (residues 615−632), 13 cytosolic amino acids closest to the membrane, and 5 amino acids from the transmembrane region. Cadherins are single transmembrane-spanning glycoproteins of about 700 amino acids. pVEC has been shown to translocate efficiently into cells of different cell lines by a receptor-independent mechanism and to be able to carry macromolecular cargoes across plasma membranes (*11*, *32*). Whereas pVEC exhibits no toxicity on mammalian cells, it has been shown to possess potent antimicrobial properties (*33*). While an earlier study suggested an energy independent transport through the cell membranes (*32*), recently strong evidence for an endocytic uptake mechanism of pVEC has been brought up (*12*). The paradigm shift from an energy independent, direct transport of CPPs through biomembranes, as postulated in earlier studies to concepts involving endocytosis (*2*, *17*, *34*−*37*), reflects a general trend in the CPP area.

W2-pVec was initially designed to allow Trp-fluorescence studies, without largely changing the properties of pVEC. In fact, we demonstrated in a previous study that both peptides possess very similar physicochemical properties, despite the desired fact of an increased affinity of W2-pVEC toward membrane interfaces (*38*).

In a time-lapse AFM study under conditions close to physiological, we were able to demonstrate for the first time a CPP-induced time- and concentration-dependent transformation process of DPPC domains without compromising the bilayer integrity. Both pVEC and W2-pVEC were able to transform the DPPC gel phase domains, which initially protruded by 1 nm from the DOPC phase, via an intermediate state of branched structures into a physical state that was indiscernible from the DOPC liquid-crystalline phase. Fluorescence polarization experiments revealed that these effects may be caused by the peptides' capacity to increase the fluidity of the DPPC domains. Interestingly, gel phase domains composed of sphingomyelin (SM) were not significantly affected by these peptides.

## MATERIALS AND METHODS

*Materials.* The VE-cadherin-derived peptides were synthesized by NMI Peptides, Reutlingen, Germany. The peptides were N-terminally amidated, and their identity and purity (>98%) were controlled by mass spectral and HPLC analysis. The analytical data were as follows: pVEC (LLIILRRRIRKQAHAHSK-$NH_2$), $mass_{calc}$ 2207.4 Da, $mass_{exp}$ 2207.0 Da; W2-pVEC (LWIILRRRIRKQAHAHSK-$NH_2$), $mass_{calc}$ 2280.4 Da, $mass_{exp}$ 2280.2 Da. 1-Palmitoyl-2-oleoyl-phosphatidylcholine (POPC), 1,2-dipalmitoyl-phosphatidylglycerol (DPPC), 1,2-dioleoyl-phosphatidylglycerol (DOPC), and sphingomyelin (egg, chicken) were purchased from Avanti Polar Lipids (Alabaster, AL), of the best quality available, and used without further purification. Analytical grade $CaCl_2 \cdot 2H_2O$, methanol, and chloroform were purchased from Merck (Darmstadt, Germany); calcein, NaCl, EDTA, phosphate buffered saline (PBS), and HEPES were from Fluka (Buchs, Switzerland). 1,6-Diphenyl-1,3,5-hexatriene (DPH) was purchased from Molecular Probes (Leiden, The Netherlands).

*Preparation of Calcein Containing Large Unilamellar Vesicles.* For the calcein leakage studies, large unilamellar vesicles (LUVs) were prepared by dissolving the phospholipids, either pure or in the desired molar ratio, in chloroform to ensure complete dissolution and mixing of the components. The lipid solution was dried at 37 °C in a rotary evaporator to yield a thin film of the lipids, and then kept under high vacuum overnight. The dry film was then redispersed in buffer (20 mM calcein, in PBS pH 7.4, containing 1 mM EDTA for complexation of $Ca^{2+}/Mg^{2+}$ to avoid interference with calcein fluorescence), and the resulting multilamellar vesicle (MLV) dispersion was treated by five freeze−thaw cycles in liquid nitrogen and water at 37 °C. LUVs were then obtained by extruding four times through 0.4 $\mu$m and eight times through 0.1 $\mu$m Nuclepore polycarbonate membranes (Sterico, Wangen, Switzerland) by means of a Lipex extruder (Vancouver, Canada) (*39*). A plastic syringe (5 mL volume, plugged with a filter pad) mounted in a centrifugation tube was filled with hydrated Sephadex G-50 gel. After spinning at 2000 rpm for 3 min the gel column had dried

and separated from the sides of the syringe. To remove untrapped dye 1 mL of the LUV dispersion was dropped onto the dry gel bed, and the liposomes were eluted by centrifugation at 200*g* for 3 min (*40*). To ensure the quality of the liposomes, the particle size distribution of the LUVs was checked by photon correlation spectroscopy on a Zetasizer 3000HSA (Malvern Instruments Ltd, Malvern, U.K.). Lipid concentration was determined by an enzymatic colorimetric test for phospholipids as obtained from Roche Diagnostics (Mannheim, Germany).

*Calcein Leakage Tests.* Using 96-well plates (Nunc, Wiesbaden, Germany) 50 $\mu$L of a 400 $\mu$M LUV dispersion was mixed with 50 $\mu$L of peptide solutions of different concentrations. Calcein leakage from vesicles was monitored fluorimetrically by measuring the decrease in self-quenching (excitation at 462 nm, emission at 525 nm) after 60 min at room temperature on a Varian Cary Eclipse spectrofluorometer (Mulgrave, Australia). The buffer blank was subtracted from all values and the fluorescence intensity corresponding to 100% leakage was determined after addition of Triton X-100 (*41*). Results were displayed as percentage of maximum leakage.

*Preparation of Phase-Separated Supported Phospholipid Bilayers.* We made phase-separated SPBs by direct fusion of vesicles onto a mica surface (*42*). We followed in principle the same protocol described above for calcein containing LUVs except for using HEPES buffer pH 7.4 instead of calcein containing PBS buffer pH 7.4. As lipids we used mixtures of DOPC with DPPC (1:1) or SM (3:2) and HEPES buffer. During the whole process temperature was kept at 65 °C. LUVs were deposited on a freshly cleaved mica disk, which was glued on a steel disk with epoxy adhesive, then inserted into a 13 mm Swinney filter chasing (Millipure, Bedford, MA), and incubated in a water bath at 65 °C. The phase-separated SPBs were left at room temperature for at least 12 h, but not more than 24 h, before being rinsed 15 times with sterile filtrated HEPES buffer to remove unfused LUVs. The bilayers were carefully protected from desiccation and kept in a moist chamber at room temperature prior to AFM imaging.

*AFM Imaging.* The AFM studies were performed on a Nanoscope IIIa MultiMode AFM (Digital Instruments, San Diego, CA) equipped with an "E" (16 $\mu$M) or a "J" (120 $\mu$M) scanner. The bilayers on mica disks were installed into a contact mode fluid cell (Digital instruments) and recorded in the contact mode using oxide-sharpened silicon nitrate tips mounted on triangular cantilevers with a nominal spring constant of 0.06 N/m at scanning rates of 1.5 to 3 Hz. The scan angle was 90° and the force used was maintained at the lowest possible value by continuously adjusting the set point during imaging. After having imaged the blank bilayers the HEPES buffer was replaced by a 5 $\mu$M or 10 $\mu$M solution of the respective peptide. The bilayers were carefully protected from desiccation by maintaining a thin layer of buffer prior to addition of peptide solution. The experiments were performed without an O-ring. The exchange of buffer by peptide solution was in order to have better control of the concentration of the peptide, and to minimize peptide consumption. All experiments were performed at room temperature (22 °C). Data processing was restricted to flattening (first or second order, *Nanoscope Reference Manual*, 1998). For every experiment at least three different parts of at least two independent samples were inspected.

*Fluorescence Polarization.* LUVs were prepared from DPPC according to general protocol described for calcein containing LUVs. Lipid concentration was determined by an enzymatic colorimetric test for phospholipids (MPR 2) obtained from Roche Diagnostics (Mannheim, Germany), and adjusted to 50 $\mu$M. DPH was added from a 1 mM stock solution in tetrahydrofuran to LUVs composed of 50 $\mu$M DPPC to give a final concentration of 100 nM (probe/lipid molar ratio 1:500). Liposomes were used between 30 min and 8 h after addition of DPH. Prior to the measurement 300 $\mu$M peptide from a 1 mM stock solution was added and allowed to equilibrate for 15 min. Fluorescence polarization was measured on a Varian Cary Eclipse spectrofluorometer (Mulgrave, Australia). All measurements were made in 10 mm wide 40 $\mu$L microcuvettes using a multicell Peltier device connected to a temperature controller. Measurements started at 55 °C, and temperature was gradually lowered to 15 °C. After a desired temperature was reached, the sample was allowed to equilibrate for 5 min. Fluorescence was excited at 340 nm and the emission was determined at 452 nm; for each sample five measurements were performed and averaged. A polarization attachment (Varian, Mulgrave, Australia) was adapted to the Varian Cary Eclipse spectrofluorometer. Steady-state fluorescence polarization $P$ was determined according to the following equation (*43*):

$$P = \frac{I_{VV} - GI_{VH}}{I_{VV} + GI_{VH}} \quad (1)$$

where $I_{VV}$ is the emission intensity of vertically polarized light parallel to the plane of excitation, and $I_{VH}$ is the emission intensity of horizontally polarized light perpendicular to the plane of excitation. The instrumental factor $G$ ($G = I_{HV}/I_{HH}$) was determined by measuring the polarized components of the probe's fluorescence at horizontally polarized excitation.

*Dynamic Light Scattering (DLS).* Size and polydispersity of a 50 $\mu$M LUV dispersion alone or after addition of 300 $\mu$M peptide were monitored at 25 °C and 50 °C over a period of 30 min by dynamic light scattering (DLS) at a scattering angle of 90° on a Malvern Zetasizer 3000HS (Malvern Instruments Ltd, Malvern, U.K.) which was equipped with a He−Ne ion laser (633 nm). Hydrodynamic diameters ($d_H$, nm) were calculated from the diffusion coefficient $D$ using the Stokes−Einstein equation:

$$d_H = \frac{kT}{3\pi\eta D} \quad (2)$$

where $k$ is the Boltzmann constant, $T$ the absolute temperature (K), and $\eta$ the viscosity (mPa·s$^{-1}$) of the solvent. The correlation function was analyzed by the CONTIN method, and the intensity distribution was chosen for evaluation of the data.

*Circular Dichroism (CD) Measurements.* Circular dichroism was measured on a Jasco J720 spectropolarimeter (Jasco, Tokyo, Japan) at 25 °C using a 0.2 mm quartz cell. All spectra were recorded between 190 and 250 nm and corrected for background contributions. The peptide concentration was

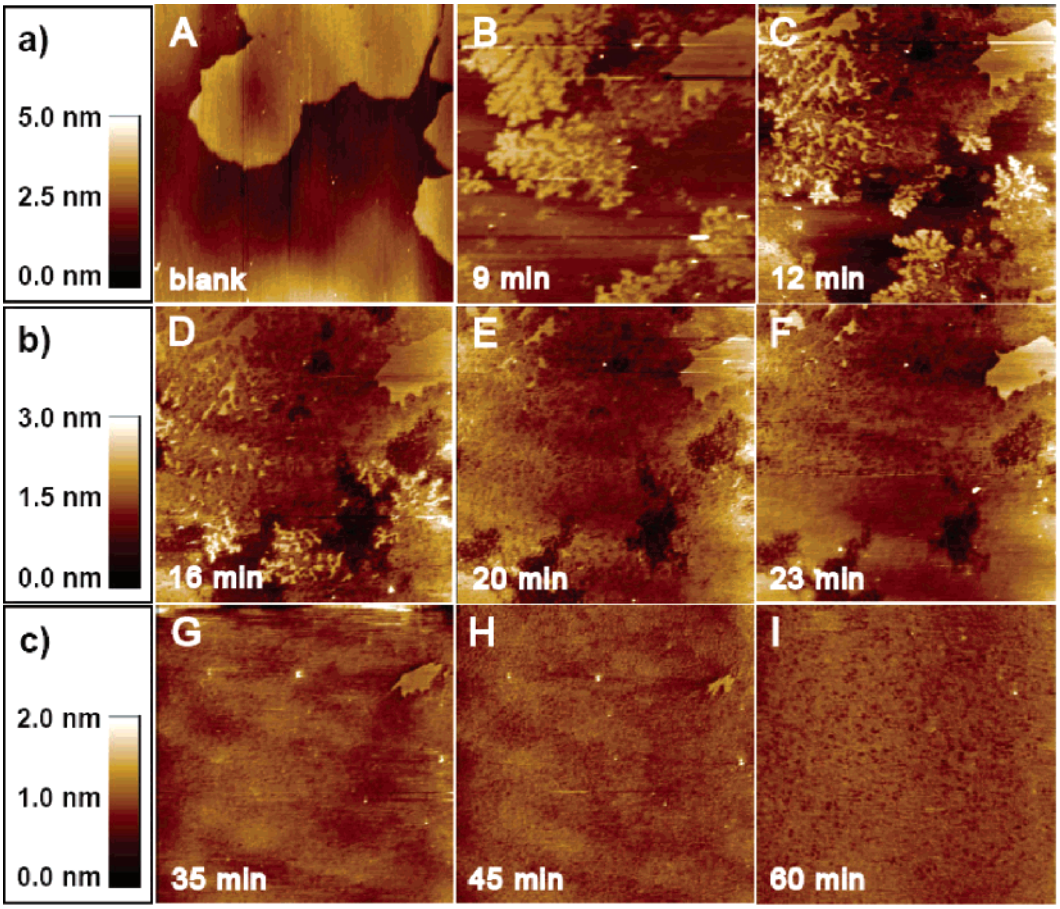


FIGURE 1: AFM scans of the time dependent transformation of DPPC gel phase domains upon addition of W2-pVEC. A 10 $\mu$M solution of W2-pVEC in HEPES pH 7.4 was added to a phase-separated SPB composed of DOPC and DPPC (1:1). The defined part was observed for 60 min. The scale for the A−H scans is 5 $\mu$m × 5 $\mu$m; scan I is shown in higher magnification (2 $\mu$m × 2 $\mu$m). Height scale a applies to scans A and B, scale b to scans C−F, and scale c to scans G−I.

20 $\mu$M in a 5 mM PBS buffer, pH 7.4. For micelle formation DPC in a concentration of 2.5 mM was used. The results were expressed as mean residue ellipticities, $[\theta]_{MR}$ (deg cm$^2$/dmol).

## RESULTS

*AFM Imaging. Effects of pVEC and W2pVEC on DOPC/DPPC Bilayers.* Fusion of unilamellar vesicles on freshly cleaved mica resulted in phase-separated SPBs. After careful and extensive rinsing with sterile filtrated HEPES buffer, clean bilayers were obtained (Figures 1A and 2A). Occurrence of unfused liposomes was sporadic. The round-shaped DPPC domains with diameters ranging from 0.3 to 3 $\mu$m protruded by approximately 0.8 to 1.0 nm out of the DOPC fluid phase. When we replaced the HEPES buffer covering the bilayer with an aqueous 10 $\mu$M, pH 7.4 W2-pVEC solution in HEPES buffer, an efficient transformation process of the DPPC gel phase was observed (Figure 1). First scans of good quality were recordable already 9 min after addition of W2-pVEC. Due to thermal drift after the replacement of the buffer, earlier observations were difficult or suffered from low resolution. The 2 to 3 $\mu$m large gel domains transformed in a time-dependent fashion. The process set on at the edges of the domains, which were increasingly pervaded by branched channels (Figure 1B,C). Especially between 12 and 23 min (Figure 1C−F) three levels differing in height by about 0.5 nm became visible. The lowest, and therefore darkest, level was understood to correspond to lipid domains in the liquid crystalline state (DOPC), whereas the uppermost and brightest level represented the domains of gel phase lipid (DPPC), which was largely unaffected by peptide-induced transformation. The intermediate level consisted of those parts of the bilayer where transformation was in process. Upon addition of W2-pVEC, only a small part of an initially large DPPC gel phase domain with a sharp borderline to the liquid crystalline phase was left after 35−45 min (Figure 1G,H). After 60 min the initially phase-separated bilayer became homogeneous (Figure 1I; compare to Figure 1A−H).

To analyze the peptide-induced transformation process further and to rule out that the peptide caused erosional damage of the bilayer, we performed a section analysis. Figure 2A shows a typical blank bilayer with DPPC gel phase domains protruding by 0.8 nm to 1.1 nm from the surface of the DOPC fluid phase. Twelve minutes after the addition of W2-pVEC those parts of the DPPC gel phase that were not yet transformed still protruded by the typical value of 0.8 to 1.1 nm from the surface, whereas in the region where the turnover took place predominantly differences of about 0.3 nm in height were found (Figure 2B). Sixty minutes after addition of W2-pVEC (Figure 2C) the bilayer was almost flat with some unevenness below 0.1 nm height, which may be attributed to the presence of peptide on the bilayer surface. The typical height of phase-separated SPBs (including a thin

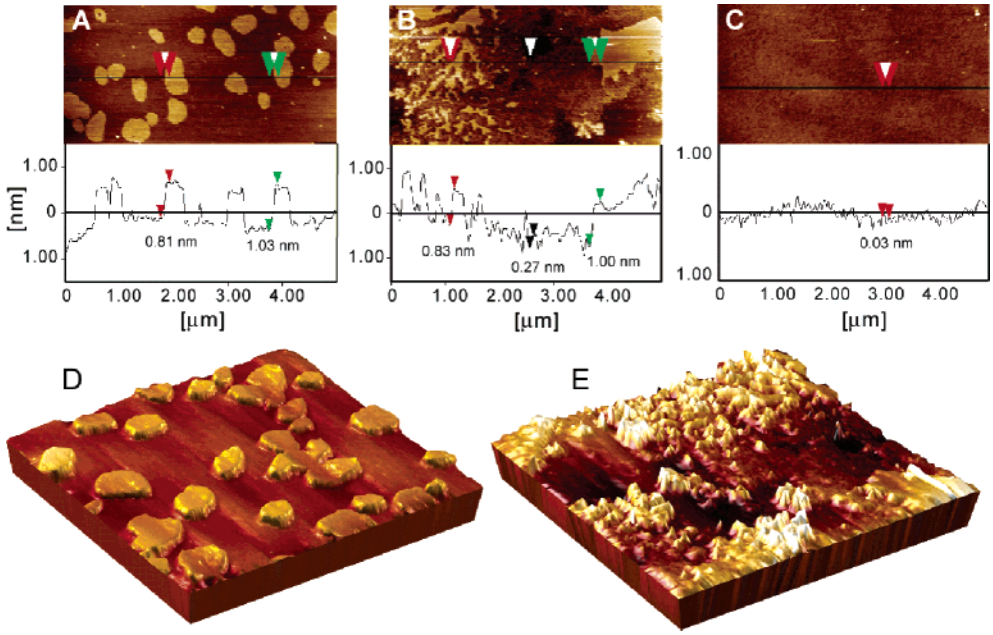


FIGURE 2: AFM scans, section analysis, and 3D representation of phase-separated SPB composed of DOPC/DPPC (1:1). A blank bilayer and its height profile obtained by a section along the indicated line (A) and bilayers 12 min (B) and 60 min (C) after addition of a 10 $\mu$M solution of W2-pVEC. The heights of the structures were estimated from AFM scans using the section analysis software provided by Digital Instruments. (D) 3D representation of Figure 2A and (E) of Figure 2B.

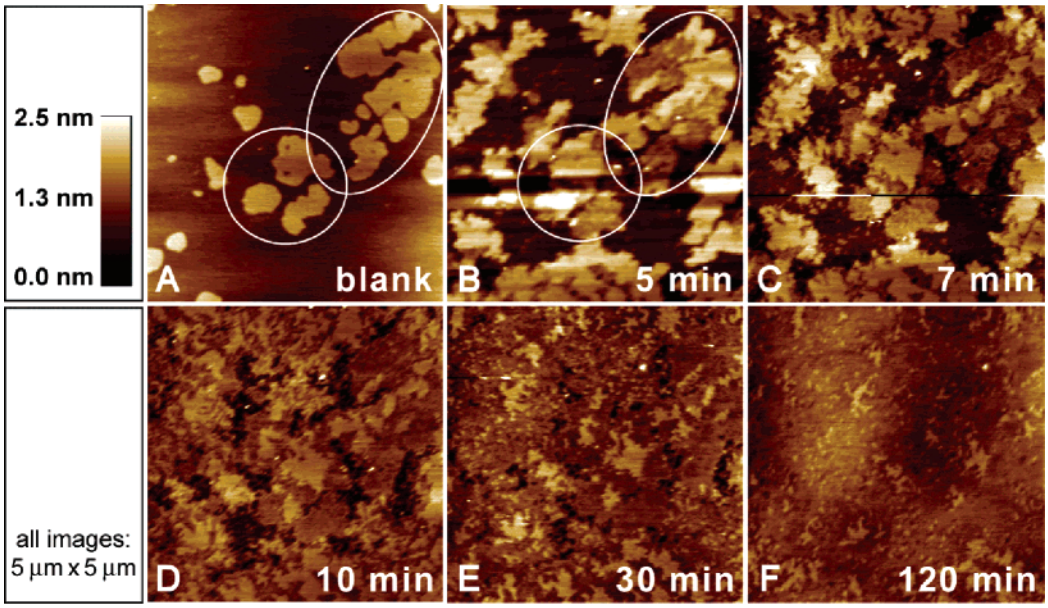


FIGURE 3: AFM scans of the time dependent transformation of DPPC gel phase domains upon addition of pVEC. A 10 $\mu$M solution of pVEC in HEPES pH 7.4 was added to a phase-separated SPB composed of DOPC and DPPC (1:1). The defined part was observed for 120 min. The scale for all scans is 5 $\mu$m $\times$ 5 $\mu$m. The height scale given in the inset applies to all scans.

layer of water between the mica surface and the lower leaflet of the bilayer) was previously found to be 5.6 $\pm$ 0.3 nm to 6.0 $\pm$ 0.2 nm (*22*, *44*, *45*), therefore approximately 6 nm deep defects would be observable in the case of bilayer damage by erosion. In fact, we found no such defects in any of the scans. Figure 2 represents three-dimensional representations of a blank DPPC/DOPC phase-separated SPB (Figure 2D) and of a phase-separated SPB of the same composition but 12 min after addition of 10 $\mu$M W2-pVEC (Figure 2E).

When a 5 $\mu$M instead of 10 $\mu$M W2-pVEC solution was added to the phase-separated SPB, the same phenomena could be observed but the turnover process occurred markedly more slowly (Figure II, Supporting Information).

Figure 3 shows the effects of a 10 $\mu$M pVEC solution on a DPPC/DOPC SPB. After addition of the peptide, the previously distinct DPPC domains of the blank bilayer (Figure 3A) expanded and spread into the fluid DOPC phase (Figure 3B). At the borders between gel and fluid phase again branched structures could be observed (Figure 3C−E), although this phenomenon was less pronounced as compared to W2-pVEC solutions. Again, in particular between 7 and 30 min (Figure 3C−E), three distinct levels were visible. After 120 min (Figure 3F) an almost flat bilayer with regularly distributed, small domains remained. The section analysis of the bilayer revealed that, as compared to the blank bilayer (Figure 4A), the differences in height of the domains increased shortly after addition of pVEC (Figure 4B,C). After

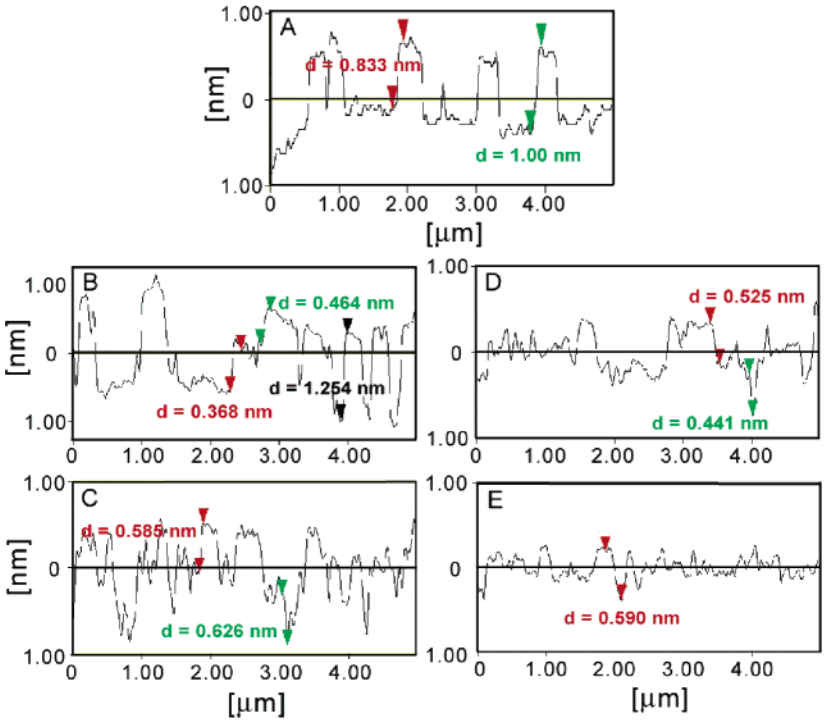


FIGURE 4: AFM section analysis of phase-separated SPB composed of DOPC/DPPC (1:1) upon pVEC treatment. Height profiles obtained by cross sections of a blank bilayer (A), 5 min (B), 10 min (C), 45 min (D), and 120 min (E) after addition of a 10 $\mu$M pVEC solution. The heights of the structures were estimated from AFM scans using the section analysis software provided by Digital Instruments.

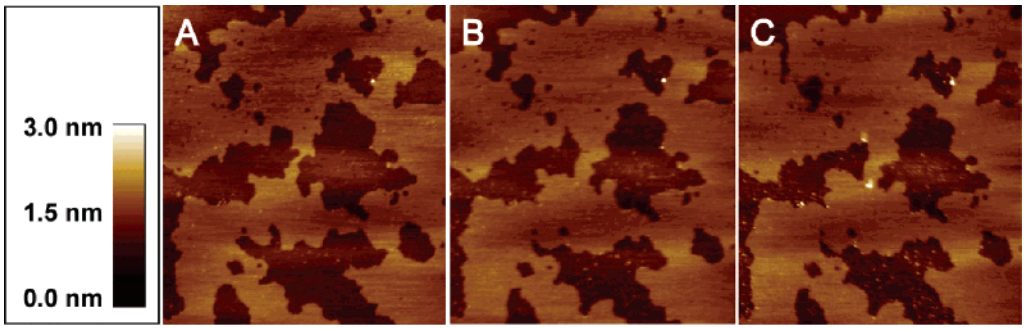


FIGURE 5: AFM scans of a POPC/SM bilayer before (A), 15 min after (B), or 90 min after (C) addition of 10 $\mu$M solution of pVEC. The scale for all scans is 5 $\mu$m $\times$ 5 $\mu$m. The height scale given in the inset applies to all scans.

45 min (Figure 4D), the differences flattened out, and after 120 min (Figure 4E), a more regular surface structure with only small differences in height was observed to develop. Generally, the effects induced by pVEC were similar to those of W2-pVEC but the process was slower and somewhat less efficient. Similarly to W2-pVEC, lowering the concentration of the pVEC solution to 5 $\mu$M resulted in a slower transformation of the bilayer (Figure I, Supporting Information).

*Effects of pVEC and W2pVEC on DOPC/SM Bilayers.* To investigate whether the peptide-induced transformation processes were specific for glycerophospholipids, we also studied phase-separated SPBs where DPPC was replaced by egg SM, having a phase transition temperature ($T_m$) similar to that of DPPC. Egg SM consists of fully saturated fatty acids only, namely, 84% palmitic acid and small amounts of longer chain saturated fatty acids (*46*). For palmitoyl SM a $T_m$ of 37.5 °C has been determined (*47*), and for the complete egg SM a $T_m$ of 38 °C (*48*). As compared to DPPC gel phase domains, SM domains were generally somewhat less regular and showed mostly diameters above 1 $\mu$m (Figure 5A). As shown in Figure 5B,C, neither 15 min nor 90 min after addition of 10 $\mu$M W2-pVEC could significant changes in the domain structure be observed. After 90 min we observed sporadic small dots on the SPB surface, which may represent aggregated peptide (Figure 5C). Also 10 $\mu$M pVEC exhibited no significant effects on DOPC/SM SPBs over a period of 120 min (data not shown).

*Peptide Effects on Bilayer Integrity. Calcein Leakage Experiments.* Previous in vitro studies showed that pVEC concentrations up to 20 $\mu$M did not increase (Bowes cells) or only very slightly increased (bEnd and AEC cells) membrane permeability (*32*). Furthermore, it has been demonstrated that pVEC permeabilize microbial cells at concentrations that cannot cause damage to mammalian cells (*33*). In order to test whether pVEC could permeabilize pure phospholipid membranes, and whether the modification in W2-pVEC may affect lipid membrane integrity, we performed a dye leakage assay with calcein loaded POPC LUVs. In Figure 6 we compare membrane permeabilizing effects of increasing concentrations of pVEC, W2-pVEC, and melittin as control in a 200 $\mu$M solution of neutral POPC LUVs at pH 7.4. Melittin, a basic, amphipathic 26-amino acid peptide, which has the propensity to form pores in lipid

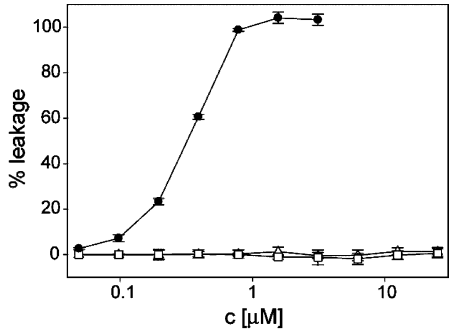


FIGURE 6: Percent leakage of LUV entrapped fluorescent calcein as a function of peptide concentration. Peptide solutions up to a final concentration of 25 $\mu$M were added to a 400 $\mu$M POPC LUV dispersion in PBS buffer, pH 7.4. From the increase in calcein fluorescence the peptide-induced leakage in percent was calculated for melittin (●), pVEC (△), and W2-pVEC (□). Data were recorded after 120 min incubation at ambient temperature (approximately 22 °C) and are represented as mean ± SD ($n$ = 3).

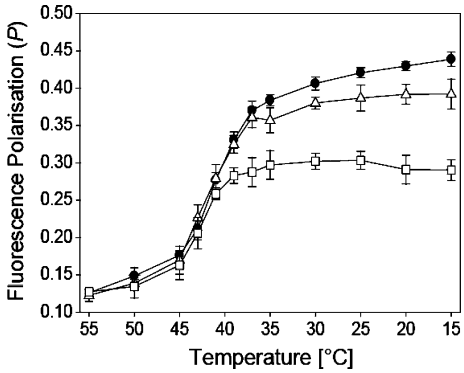


FIGURE 7: Fluorescence polarization of 100 nM DPH incorporated in 50 $\mu$M DPPC LUVs as a function of the temperature. A blank dispersion of DPPC LUVs (●) was compared with LUVs containing 300 $\mu$M solutions of the peptides pVEC (△) and W2-pVEC (□). Results are represented as means ± SD ($n$ = 3).

bilayers (*49*), led to a complete leakage at a concentration as low as 1 $\mu$M. Up to peptide concentrations of 25 $\mu$M neither pVEC, nor W2-pVEC caused any significant leakage. These concentrations were largely above those used in the AFM experiments, which were 5 $\mu$M and 10 $\mu$M.

*Fluorescence Polarization.* To scrutinize whether the effects of the investigated peptides on the DPPC gel phase domains can in fact be explained by a shift in the phase transition temperature ($T_m$) and/or the viscosity of the gel phase, we performed a fluorescence polarization study. For this purpose the polarization of the membrane-bound fluorophore DPH was used to monitor the internal microviscosity of DPPC bilayers as a function of the temperature. DPH is nonfluorescent in aqueous dispersion but partitions readily into the hydrophobic core of lipid membranes owing to its high lipid−water partition coefficient $K_p$ of 1.3 × $10^6$, associated with a strong increase in fluorescence intensity (*50*). A temperature scan of blank DPPC LUVs showed an increase in fluorescence polarization from 0.13 at 55 °C to 0.44 at 15 °C with a phase transition temperature of about 40 °C (Figure 7). This is in good agreement with a previous differential scanning calorimetry study of DPPC that found a phase transition temperature at 41 °C (*51*). In the presence of 300 $\mu$M pVEC the profile of the curve was identical with that of blank LUVs up to the region where phase transition occurs, whereas the microviscosity of the gel phase was

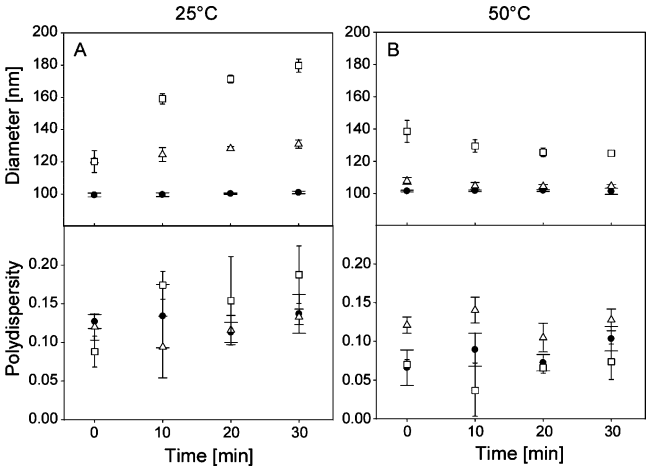


FIGURE 8: Diameters and polydispersity indices of size distributions of 50 $\mu$M DPPC LUVs without and with peptide monitored over 30 min. A blank dispersion of DPPC LUVs (●) was compared with LUVs containing 300 $\mu$M solutions of the peptides pVEC (△) and W2-pVEC (□). Experiments were performed in triplicate. SD error bars of DPPC blanks are shown with long, of pVEC with medium, and of W2-pVEC with short caps.

reduced, as shown by maximum polarization degree of 0.39 as compared to 0.44 at 15 °C. W2-pVEC caused an even stronger reduction in gel phase microviscosity with a maximum polarization of only 0.29. Again, at higher temperatures, where DPPC is in the liquid crystalline state, no differences were observed. When the peptide concentration was reduced to one-half, the effect of W2-pVEC was also cut down to one-half; pVEC had no significant effect. Generally, the peptides caused no significant changes in phase transition temperature but led to a pronounced decrease in gel phase viscosity at higher concentrations.

*Dynamic Light Scattering (DLS).* Although no indications for peptide-induced damage on the bilayers could be found by AFM analysis, we performed a DLS analysis to investigate whether the integrity of LUV could be compromised at high concentrations of the investigated peptides. At 25 °C (Figure 8A) the diameters of blank LUVs increased minimally over time from 99.4 nm ± 1.2 to 100.6 nm ± 0.8 at 30 min. With mean diameters of 120 nm immediately after addition of the peptides, LUVs increased in size to 131 nm for pVEC and 179 nm for W2-pVEC. To decide whether the increase in mean diameter was (i) due to insertion and/or association of the peptide into or onto the LUV bilayers or (ii) owed to a peptide-induced turnover and damage of the vesicles, we also monitored the polydispersity index of the size distribution. In case of insertion or association, an increase in the LUV mean diameter would be expected, whereas polydispersity should be largely unchanged. In the case of compromised LUV integrity a formation of larger and/or smaller liposomes and, hence, a broader distribution and higher polydispersity could be envisaged. Also aggregation could lead to increased polydispersity. As shown in the lower panel of Figure 8A, there is only a slight tendency toward higher polydispersity after addition of W2-pVEC, but none of the peptides caused significant changes ($p$ > 0.1 throughout).

As shown in Figure 8B, at 50 °C, i.e., in the fluid phase, the DPPC LUVs had diameters of 107.8 ± 2.1 nm immediately after addition of pVEC which then stabilized at about 104 nm. For W2-pVEC LUVs, diameters were highest

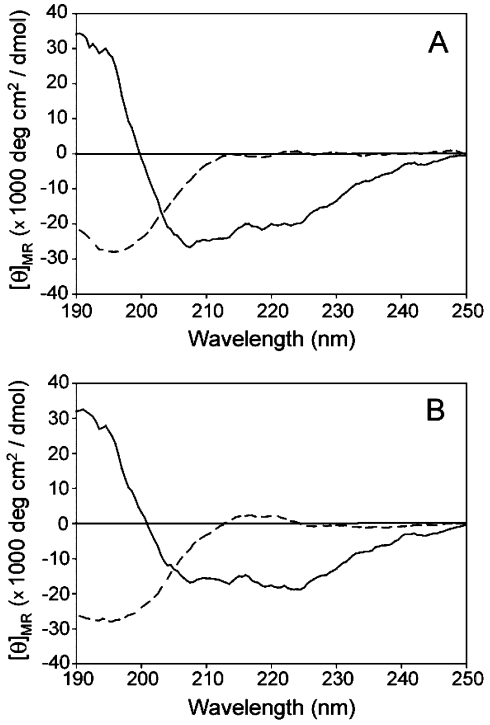


FIGURE 9: CD spectra of 20 $\mu$M solutions of pVEC and W2-pVEC in different media. pVEC (A) and W2-pVEC (B) in buffer (dashed line) and in the presence of DPC micelles (2.5 mM, peptide/lipid ratio = 0.008) (solid line). The spectra were recorded at 25 °C and the buffer was 5 mM PBS pH 7.4 in all cases.

immediately after addition (138.5 ± 6.8 nm) and then dropped to 124.9 ± 1.3 nm. Polydispersity indices ranged from 0.037 to 0.140. At $t = 0$ there was a significant difference in polydispersity between untreated and pVEC treated LUVs ($p < 0.02$), which disappeared over time. LUVs treated with W2-pVEC were never significantly different from the untreated ones ($p > 0.1$ in all cases). This provides evidence for association or integration in the bilayer rather than for any form of turnover or damage to the membrane.

*Circular Dichroism (CD) Measurements.* In aqueous buffer solution (PBS, 5 mM, pH 7.4) pVEC as well as W2-pVEC show CD spectra with a single minimum at about 198 nm, characteristic for a nonordered structure (dashed lines in Figure 9). However, in the presence of an excess of DPC micelles, a marked induction of secondary structure was observed for both peptides (solid lines in Figure 9). The spectra with maxima at 190−195 nm and minima at 205 nm associated with a shoulder around 220 nm indicate a tendency to adopt, at least in part, an α-helical conformation (*52*). For pVEC (Figure 9A) the evidence for α-helicity was slightly better than for W2-pVEC (Figure 9B).

## DISCUSSION

In this study we show for the first time that selected CPPs, namely, pVEC and W2-pVEC, are capable of transforming DPPC gel phase domains of phase-separated SPBs into a less ordered state with lower microviscosity. Right after the peptides were added to the SPBs, the transformation process set in, starting at the edges of the DPPC gel phase domains. From here, an erosion process began, with branched channels of already transformed zones penetrating into the center of the gel phase domains. The larger the DPPC domains, the more time was required for complete transformation. Mechanistically, disruptions of the interactions between the lipid polar headgroups due to the intercalation of the CPP and hence a less tight packing of the gel phase DPPC domains seem to be responsible for their progressive disappearance. This hypothesis is supported by fluorescence polarization results, which demonstrated that the peptides interact with DPPC membranes in the gel phase state. Moreover, the increase in vesicle diameters upon addition of the two CPPs as observed in the DLS studies indicates that the peptide interacts with DPPC, either by integration into the bilayer interface or by association on the surface. The result is also in agreement with a previous study where we observed a high affinity of pVEC and W2-pVEC toward fluid phase POPC LUVs as indicated by a high partition coefficient with a log $D$ of about 3 (*38*).

In general, pVEC and its modification W2-pVEC showed very similar effects. However, the transformation induced by W2-pVEC was faster and more efficient: At a concentration of 10 $\mu$M the bilayer was completely transformed within 60 min, whereas transformation caused by 10 $\mu$M pVEC was equally intensive, but could not lead to an entirely completed transformation after 2 h. This is consistent with the higher potential of W2-pVEC to lower the microviscosity of DPPC bilayers above the phase transition temperature, which was determined by fluorescence polarization. The observed increase in affinity toward phospholipid bilayers corresponds well with experimentally determined free energies for the transfer of whole amino acids from bulk solution into the membrane−water interface or into the hydrophobic interior, which are −0.31 and −1.85 kcal/mol for the transfer into the interface ($\Delta G_{wif}$) and −1.12 and −2.09 kcal/mol into the hydrophobic interior ($\Delta G_{oct}$), for Ile (unmodified pVEC) and Trp (W2-pVEC) residues, respectively (53).

*Mechanistic Considerations for Gel Phase Transformation.* Derived from our observations we propose the following model for the molecular reorganization induced by the investigated peptides (Figure 10): Before addition of peptide, the DPPC gel phase protrudes—due to its extended acyl chains—by about 1.0 nm from the DOPC fluid phase (Figure 10A). Over time, with increasing penetration of peptide into the DPPC phase, the lipids of the gel phase transform into a less ordered state of lower microviscosity. Often, an intermediate phase, approximately 0.5 nm above the DOPC phase, but about 0.5 nm below the original DPPC domains (Figure 10B), appears to occur. This may be caused by the fact that at first only the upper lipid leaflet is affected by the peptides, before the entire bilayer will be transformed. In this final state the former gel phase DPPC domains are indiscernible from the liquid crystalline DOPC phase (Figure 10C). The hypothesis of this transformation process is strongly supported by (i) the fact that DPPC bilayers in the fluid state were 3.7 nm in height (*54*) and, therefore, 1 nm less than in the gel state (4.7 nm) (*55*), (ii) the peptides' capability to decrease the microviscosity of the DPPC gel phase, as demonstrated by fluorescence polarization, and (iii) the fact the peptides induce neither visible disintegration of the SPBs nor calcein leakage out of the LUVs. In a previous study we demonstrated that pVEC and W2-pVEC were preferably localized in the interface of phospholipid bilayers (*38*). As suggested in Figure 10C, interfacial insertion may cause a disruption of the tight molecular packing of the DPPC

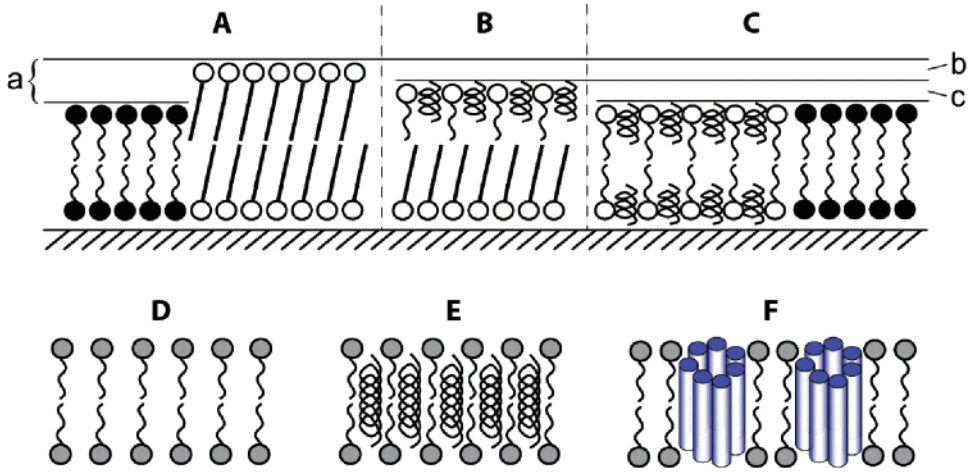


FIGURE 10: Proposed model for the molecular organization of DOPC/DPPC bilayer with and without pVEC/W2-pVEC incorporated. Blank DOPC/DPPC SPBs (A) are characterized by DPPC lipids (open headgroups) with tilted, extended acyl chains, whereas acyl chains of DOPC lipids (filled headgroups) are less ordered. This results in a height difference of about 1 nm (a). After addition of the peptides, in an intermediate state, first the upper lipid leaflet is transformed to a less ordered state by interaction with the peptides (B). In this state the bilayer is about 0.5 nm lower (b) than the unaffected DPPC and 0.5 nm higher (c) than DOPC. Finally, the whole DPPC bilayer is transformed to a less ordered and more fluid state (C) of the same height as DOPC. In contrast, when inserting in a bilayer in the fluid state (D), membrane-spanning peptides and proteins lead to a restriction of acyl chain mobility and therefore an increase in fluorescence polarization. This insertion may occur in the form of single molecules (E) or oligomeric pores (F) formed by barrel-stave type peptide association.

molecules near the headgroup region and lead to an increased flexibility of the acyl chains and, therefore, to a decreased microviscosity. In addition to that, the peptides may decrease the line tension between the DPPC gel phase and the DOPC fluid phase which causes the observed erosion of the DPPC gel phase domains and the resulting homogeneity of the bilayer. The capability of pVEC and W2-pVEC to *decrease* the viscosity of lipid bilayers below the phase transition temperature reflects a mode of interaction with phospholipid bilayers different from effects observed for cationic amphiphilic drugs or peptides and proteins, which insert into the hydrophobic core of membranes. These α-helical membrane-spanning proteins such as the C-terminal domain of the pro-apototic protein Bak (*56*), the Pf1 coat protein (*57*), and the C-terminal domain of the antiapoptotic protein Bcl-2 (*58*) *increase* the viscosity and hence the fluorescence polarization of phospholipid bilayers.

Interestingly, the amphipathic peptide ApoE, which is capable of causing fluidification of lipid bilayers, has recently been shown to cause slight erosions of DPPC domains in the presence of 1.7% trifluoroethanol (*59*). As also illustrated in Figure 10, membrane-spanning proteins, independently of insertion as single molecules (Figure 10E) or as oligomeric pores according to a barrel-stave model (*60*) (Figure 10F), would restrict the motion of lipid molecules, decrease their acyl chain flexibility, and, hence, increase the microviscosity as compared to a blank bilayer (Figure 10D). Several of these membrane-spanning peptides have been shown to destabilize unilamellar vesicles inducing leakage of an encapsulated dye (*56*, *58*), whereas neither pVEC nor W2-pVEC induced any kind of membrane damage, indicating a mild form of membrane perturbation. Whether this would result in lower toxicity when used in living systems has yet to be demonstrated.

*Related Reorganization Phenomena in Lipid Bilayers.* Several amphiphilic cationic drugs have been shown to be able to lower the phase transition temperature of DPPA (*61*) and DPPC (*62*) lipids. Although in those cases the mode of interaction was different from that for pVEC and W2-pVEC, where not the phase transition temperature but the viscosity of the gel phase was decreased, a similar effect on phase-separated supported bilayers was observed for the antibiotic azithromycin. Berquand et al. (*63*) showed that a 1 mM concentration of the amphiphilic and cationic azithromycin induced progressive erosion of DPPC domains of DOPC/DPPC SPBs, resulting in an almost flat bilayer after 60 min. Unlike pVEC, no intermediate branched structures were observed. Instead, the borders of the domains remained smooth during the entire transformation process. Another major difference was that a 100 times higher concentration than in our study was required to induce DPPC transformation. In an ensuing study (*64*), Berquand et al. found that, similarly to the CPPs in the present study, azithromycin did not alter the permeability of lipid vesicles of different composition. Also their observations that azithromycin increased the fluidity of the interface of DPPC:DOPC and DPPE:DOPC (but not SM:DOPC and SM:cholesterol:DOPC) vesicles correspond to our findings. Interestingly, again similar to our observation that SM domains were unaffected by the peptides, Berquand et al. found that, in contrast to DPPC domains, azithromycin could not significantly transform SM domains. Although this difference may surprise at first sight, since both lipids have the same polar headgroup, there are specific features in the molecular structure of SM which may account for its particular stability against physical transformation: The amide and hydroxyl groups in the interface of SM can act as both hydrogen bond donors and acceptors, whereas the amide carbonyl provides an additional hydrogen acceptor. This interfacial peculiarity gives SM the unique ability to form both strong intra- and intermolecular hydrogen bonds (*65*). In contrast, phosphatidyl cholines with two ester carbonyls in this region have only hydrogen bond accepting features. The stronger interactions in the interface of SM result in closer lipid packing, better chain stacking, membrane stabilization, and lower membrane permeability (*66*). Therefore, we conclude that the resistance of SM domains against transformation by the peptides as demonstrated in our studies reflects tighter lipid packing owing to

stronger intermolecular interactions between SM lipids as compared to DPPC lipids.

Relative to our work we would also like to briefly discuss both similarities and distinct differences in two other phenomena of reorganization of phospholipid bilayers: namely, the formation of highly ordered, striated domains in SPBs induced by transmembrane peptides and the induction of interdigitated domains in gel phase bilayers, which can be caused by different solvents and chemicals and also by physical pressure or heat.

The formation of striated domains in gel phase lipids of SPBs was first reported by Rinia et al. (*26*); they were induced by hydrophobic, α-helical transmembrane peptides—so-called WALP peptides—preferably at peptide concentrations between 2 and 10 mol %. The striated domains were characterized by line-type depressions consisting of peptide arrays, which appeared about 0.3 nm below the surface of unaffected bilayer areas. The depressions were flanked by elevated areas 0.1 nm to 0.3 nm higher than the bilayer, which are probably the result of packing constraints caused by the included peptide and lead to less tilt in the lipids' acyl chains. At high peptide concentrations (10 mol %), large parts of the bilayer were covered by striated domains with a repeat distance of 7.6 nm, forming an extremely ordered, mainly hexagonal pattern characterized by angles of 120°. Although also the WALP peptides caused transformation of DPPC SPBs, four characteristic differences to our findings could be identified: (i) the depressions consisted of pure WALP peptides, instead of peptide inserted into the bilayer in our study, (ii) the difference in height was 0.3 nm as compared to 0.8 to 1.0 nm in our study, (iii) also areas higher than a blank bilayer appeared, and (iv) the transformation process led to extremely ordered, hexagonal structures, whereas rather irregular, branched structures were observed in our study. In an ensuing study, Rinia el al. (*27*) found that replacement of the Trp residues in the flanking area of WALP peptides by other uncharged amino acids caused only minimal differences in the formation of striated domains, whereas replacement by positively charged residues gave rise to completely different morphologies.

The formation of interdigitated domains represents a less specific response of phospholipid bilayers to various surface active molecules (alcohols, anaesthetics, certain proteins), which are able to replace water from the phospholipid headgroups without penetrating deep into the bilayer (*67, 68*). Whereas in a normal bilayer the tails of the lipid chains border on each other in the center of the bilayer, interdigitated bilayers are characterized by fully intercalated lipid chains. Therefore their thickness was estimated to be 1.6 nm (*67*) to 1.9 nm (*44*) less than that of normal DPPC bilayers. Two major discrepancies to our observation led us to exclude interdigitation as a possible mechanism of the peptides investigated in our study: (i) As a consequence of interdigitation, the bilayer is rigidified, and the lateral mobility within the bilayer decreased (*67, 69*), whereas we demonstrated an increased mobility of the lipids after incubation with the peptides. (ii) Furthermore, interdigitated domains differed by 1.6 nm to 1.9 nm from blank DPPC bilayers, whereas the depressions in our study differed only by 0.8 nm to 1.0 nm.

*Pharmaceutical and Toxicological Implications.* Any mechanism of translocation resulting in significant permeabilization of the membrane would be unacceptable from a pharmaceutical or toxicological point of view. The dye leakage experiments were, therefore, performed to check whether the peptide caused damage of pure phospholipid bilayers and to ensure that the insertion of a Trp in W2-pVEC would not increase the membrane permeabilization potential of the peptides. In fact, no calcein leakage was found for any of the modifications up to a concentration of 50 μM, which is well above the concentrations used in the AFM studies (5−10 μM) and the cell culture experiments, i.e., 0.5 μM (*70*) or 10 μM (*32*). Accordingly, in vitro studies showed that pVEC concentrations up to 20 μM did not increase (Bowes cells) or only very slightly increased (bEnd and AEC cells) membrane permeability (*32*). Interestingly, pVEC permeabilized bacterial cells at concentrations as low as 2 μM, which cannot cause damage to mammalian cells (*33*). This may be explained by the abundance of negative charges in bacterial membranes (*71*) together with the fact that for many cationic antimicrobial peptides an increased affinity for negative lipids has been demonstrated (*72*−*74*). The combination of efficient uptake, cellular compatibility in mammalian cells, and its antimicrobial activity renders pVEC and modifications thereof of potential interest for the treatment of intracellular infections.

## CONCLUSIONS

In this study we present time-lapse AFM observations on the effects of the two CPPs pVEC and its modification W2-pVEC on phase-separated SPBs. Both peptides induce a transformation process in the DPPC domains of the gel phase, which led via an intermediate state with branched structures to flat bilayers. In combination with fluorescence polarization experiments we revealed the capability of the investigated peptides to disrupt the tight molecular packing of the DPPC molecules and, therefore, increase the fluidity of DPPC domains as the underlying mechanism of this transformation. Owing to the particular molecular structure of their interfacial region, which allows strong hydrogen bonds and hence tighter packing, SM domains could not be affected by the peptides. In contrast to membrane-spanning peptides, which decrease the fluidity of bilayers, and in agreement with a previous study, we propose that the investigated peptides mainly interact with the bilayer interface and, therefore, lessen the packing density of acyl chains of the lipid. Evidence from AFM observations, dynamic light scattering studies, and liposome dye leakage experiments indicated that bilayer integrity was not compromised by the peptides. Our work represents the first observation of a CPP induced transformation process of phase-separated phospholipid bilayers and reveals a novel aspect to be considered to explain the cellular uptake of CPPs.

## ACKNOWLEDGMENT

The authors thank Fernanda Rossetti and Marc Dusseiller (ETH Zurich) for valuable advice concerning the AFM, Dr. Markus Birringer (ETH Zurich) for introduction into CD, and Carmen Herbig for 3D renderings.

## SUPPORTING INFORMATION AVAILABLE

Time dependent transformation of DOPC/DPPC bilayers by 5 μM solutions of pVEC and W2-pVEC. This material

is available free of charge via the Internet at http://pubs.acs.org.

## REFERENCES


1. Snyder, E. L., and Dowdy, S. F. (2004) Cell penetrating peptides in drug delivery, *Pharm. Res. 21*, 389−393.
2. Trehin, R., and Merkle, H. P. (2004) Chances and pitfalls of cell penetrating peptides for cellular drug delivery, *Eur. J. Pharm. Biopharm. 58*, 209−223.
3. Lundberg, P., and Langel, U. (2003) A brief introduction to cell-penetrating peptides, *J. Mol. Recognit. 16*, 227−233.
4. Morris, M. C., Vidal, P., Chaloin, L., Heitz, F., and Divita, G. (1997) A new peptide vector for efficient delivery of oligonucleotides into mammalian cells, *Nucleic Acids Res. 25*, 2730−2736.
5. Simeoni, F., Morris, M. C., Heitz, F., and Divita, G. (2003) Insight into the mechanism of the peptide-based gene delivery system MPG: implications for delivery of siRNA into mammalian cells, *Nucleic Acids Res. 31*, 2717−2724.
6. Morris, M. C., Depollier, J., Mery, J., Heitz, F., and Divita, G. (2001) A peptide carrier for the delivery of biologically active proteins into mammalian cells, *Nat. Biotechnol. 19*, 1173−1176.
7. Lindgren, M., Hallbrink, M., Prochiantz, A., and Langel, U. (2000) Cell-penetrating peptides, *Trends Pharmacol. Sci. 21*, 99−103.
8. Derossi, D., Chassaing, G., and Prochiantz, A. (1998) Trojan peptides: the penetratin system for intracellular delivery, *Trends. Cell Biol. 8*, 84−87.
9. Snyder, E. L., and Dowdy, S. F. (2004) Cell penetrating peptides in drug delivery, *Pharm. Res. 21*, 389−393.
10. Elmquist, A., Lindgren, M., Bartfai, T., and Langel, U. (2001) VE-cadherin-derived cell-penetrating peptide, pVEC, with carrier functions, *Exp. Cell Res. 269*, 237−244.
11. Elmquist, A., and Langel, U. (2003) In vitro uptake and stability study of pVEC and its All-D analog, *Biol. Chem. 384*, 387−393.
12. Saalik, P., Elmquist, A., Hansen, M., Padari, K., Saar, K., Viht, K., Langel, U., and Pooga, M. (2004) Protein cargo delivery properties of cell-penetrating peptides. A comparative study, *Bioconjugate Chem. 15*, 1246−1253.
13. Scheller, A., Oehlke, J., Wiesner, B., Dathe, M., Krause, E., Beyermann, M., Melzig, M., and Bienert, M. (1999) Structural requirements for cellular uptake of alpha-helical amphipathic peptides, *J. Pept. Sci. 5*, 185−194.
14. Trehin, R., and Merkle, H. P. (2004) Chances and pitfalls of cell penetrating peptides for cellular drug delivery, *Eur. J. Pharm. Biopharm. 58*, 209−223.
15. Oehlke, J., Scheller, A., Wiesner, B., Krause, E., Beyermann, M., Klauschenz, E., Melzig, M., and Bienert, M. (1998) Cellular uptake of an alpha-helical amphipathic model peptide with the potential to deliver polar compounds into the cell interior non-endocytically, *Biochim. Biophys. Acta 1414*, 127−139.
16. Lundberg, M., Wikstrom, S., and Johansson, M. (2003) Cell surface adherence and endocytosis of protein transduction domains, *Mol. Ther. 8*, 143−150.
17. Wadia, J. S., Stan, R. V., and Dowdy, S. F. (2004) Transducible TAT-HA fusogenic peptide enhances escape of TAT-fusion proteins after lipid raft macropinocytosis, *Nat. Med. 10*, 310−315.
18. Drin, G., Cottin, S., Blanc, E., Rees, A. R., and Temsamani, J. (2003) Studies on the internalisation mechanism of cationic cell-penetrating peptides, *J. Biol. Chem. 287*, 31192−31201.
19. Dufrene, Y. F., and Lee, G. U. (2000) Advances in the characterization of supported lipid films with the atomic force microscope, *Biochim. Biophys. Acta 1509*, 14−41.
20. Engel, A., Schoenenberger, C. A., and Muller, D. J. (1997) High-resolution imaging of native biological sample surfaces using scanning probe microscopy, *Curr. Opin. Struct. Biol. 7*, 279−284.
21. Milhiet, P. E., Giocondi, M. C., Baghdadi, O., Ronzon, F., Roux, B., and Le Grimellec, C. (2002) Spontaneous insertion and partitioning of alkaline phosphatase into model lipid rafts, *EMBO Rep. 3*, 485−490.
22. Mou, J., Czajkowsky, D. M., and Shao, Z. (1996) Gramicidin A aggregation in supported gel state phosphatidylcholine bilayers, *Biochemistry 35*, 3222−3226.
23. You, H. X., Qi, X., Grabowski, G. A., and Yu, L. (2003) Phospholipid membrane interactions of saposin C: in situ atomic force microscopic study, *Biophys. J. 84*, 2043−2057.
24. Reviakine, I., Bergsma-Schutter, W., Morozov, A. N., and Brisson, A. (2001) Two-dimensional crystallization of annexin A5 on phospholipid bilayers and monolayers: A solid−solid phase transition between crystal forms, *Langmuir 17*, 1680−1686.
25. Milhiet, P. E., Giocondi, M. C., Baghdadi, O., Ronzon, F., Le Grimellec, C., and Roux, B. (2002) AFM detection of GPI protein insertion into DOPC/DPPC model membranes, *Single Mol. 3*, 135−140.
26. Rinia, H. A., Kik, R. A., Demel, R. A., Snel, M. M., Killian, J. A., van Der Eerden, J. P., and de Kruijff, B. (2000) Visualization of highly ordered striated domains induced by transmembrane peptides in supported phosphatidylcholine bilayers, *Biochemistry 39*, 5852−5828.
27. Rinia, H. A., Boots, J. W., Rijkers, D. T., Kik, R. A., Snel, M. M., Demel, R. A., Killian, J. A., van der Eerden, J. P., and de Kruijff, B. (2002) Domain formation in phosphatidylcholine bilayers containing transmembrane peptides: specific effects of flanking residues, *Biochemistry 41*, 2814−2824.
28. Steinem, C., Galla, H. J., and Janshoff, A. (2000) Interaction of melittin with solid supported membranes, *Phys. Chem. Chem. Phys. 2*, 4580−4585.
29. Boichot, S., Krauss, U., Plenat, T., Rennert, R., Milhiet, P. E., Beck-Sickinger, A., and Le Grimellec, C. (2004) Calcitonin-derived carrier peptide plays a major role in the membrane localization of a peptide-cargo complex, *FEBS Lett. 569*, 346−350.
30. Schmidt, M. C., Rothen-Rutishauser, B., Rist, B., Beck-Sickinger, A., Wunderli-Allenspach, H., Rubas, W., Sadee, W., and Merkle, H. P. (1998) Translocation of human calcitonin in respiratory nasal epithelium is associated with self-assembly in lipid membrane, *Biochemistry 37*, 16582−16590.
31. This reference was deleted during revision.
32. Elmquist, A., Lindgren, M., Bartfai, T., and Langel, U. (2001) VE-cadherin-derived cell-penetrating peptide, pVEC, with carrier functions, *Exp. Cell Res. 269*, 237−244.
33. Nekhotiaeva, N., Elmquist, A., Rajarao, G. K., Hallbrink, M., Langel, U., and Good, L. (2004) Cell entry and antimicrobial properties of eukaryotic cell-penetrating peptides, *FASEB J. 18*, 394−396.
34. Lundberg, M., Wikstrom, S., and Johansson, M. (2003) Cell surface adherence and endocytosis of protein transduction domains, *Mol. Ther. 8*, 143−150.
35. Vives, E., Richard, J. P., Rispal, C., and Lebleu, B. (2003) TAT peptide internalization: seeking the mechanism of entry, *Curr. Protein Pept. Sci. 4*, 125−132.
36. Richard, J. P., Melikov, K., Vives, E., Ramos, C., Verbeure, B., Gait, M. J., Chernomordik, L. V., and Lebleu, B. (2003) Cell-penetrating peptides. A reevaluation of the mechanism of cellular uptake, *J. Biol. Chem. 278*, 585−590.
37. Foerg, C., Ziegler, U., Fernandez-Carneado, J., Giralt, E., Rennert, R., Beck-Sickinger, A. G., and Merkle, H. P. (2005) Decoding the Entry of Two Novel Cell-Penetrating Peptides in HeLa Cells: Lipid Raft-Mediated Endocytosis and Endosomal Escape, *Biochemistry 44*, 72−81.
38. Herbig, M. E., Fromm, U., Leuenberger, J., Krauss, U., Beck-Sickinger, A. G., and Merkle, H. P. (2005) Bilayer interaction and localization of cell penetrating peptides with model membranes: a comparative study of a human calcitonin (hCT) derived peptide with pVEC and pAntp(43-58), *Biochim. Biophys. Acta 1712*, 197−211.
39. Mayer, L. D., Hope, M. J., and Cullis, P. R. (1986) Vesicles of variable sizes produced by a rapid extrusion procedure, *Biochim. Biophys. Acta 858*, 161−168.
40. New, R. B. C. (1990) *Liposomes, A Practical Approach*, Oxford University Press, New York.
41. Dathe, M., Schumann, M., Wieprecht, T., Winkler, A., Beyermann, M., Krause, E., Matsuzaki, K., Murase, O., and Bienert, M. (1996) Peptide helicity and membrane surface charge modulate the balance of electrostatic and hydrophobic interactions with lipid bilayers and biological membranes, *Biochemistry 35*, 12612−12622.
42. Mou, J., Yang, J., and Shao, Z. (1994) Tris(hydroxymethyl)-aminomethane (C4H11NO3) induced a ripple phase in supported unilamellar phospholipid bilayers, *Biochemistry 33*, 4439−4443.
43. Lakowicz, J. R. (1999) *Principles of Fluorescence Spectroscopy*, 2nd ed., Kluwer Academic, New York.
44. Mou, J., Yang, J., Huang, C., and Shao, Z. (1994) Alcohol induces interdigitated domains in unilamellar phosphatidylcholine bilayers, *Biochemistry 33*, 9981−9985.

45. Grandbois, M., Clausen-Schaumann, H., and Gaub, H. (1998) Atomic force microscope imaging of phospholipid bilayer degradation by phospholipase A2, *Biophys. J. 74*, 2398−2404.
46. Wood, P. D., and Holton, S. (1964) Human Plasma Sphingomyelins, *Proc. Soc. Exp. Biol. Med. 115*, 990−992.
47. Cohen, R., Barenholz, Y., Gatt, S., and Dagan, A. (1984) Preparation and characterization of well-defined D-erythro sphingomyelins, *Chem. Phys. Lipids 35*, 371−384.
48. Wu, W. G., Chi, L. M., Yang, T. S., and Fang, S. Y. (1991) Freezing of phosphocholine headgroup in fully hydrated sphingomyelin bilayers and its effect on the dynamics of nonfreezable water at subzero temperatures, *J. Biol. Chem. 266*, 13602−13606.
49. Matsuzaki, K., Yoneyama, S., and Miyajima, K. (1997) Pore formation and translocation of melittin, *Biophys. J. 73*, 831−838.
50. Huang, Z. J., and Haugland, R. P. (1991) Partition coefficients of fluorescent probes with phospholipid membranes, *Biochem. Biophys. Res. Commun. 181*, 166−171.
51. Silvius, J. R., Read, B. D., and McElhaney, R. N. (1979) Thermotropic phase transitions of phosphatidylcholines with odd-numbered n-acyl chains, *Biochim. Biophys. Acta 555*, 175−178.
52. Greenfield, N., and Fasman, G. D. (1969) Computed circular dichroism spectra for the evaluation of protein conformation, *Biochemistry 8*, 4108−4016.
53. White, S. H., and Wimley, W. C. (1998) Hydrophobic interactions of peptides with membrane interfaces, *Biochim. Biophys. Acta 1376*, 339−352.
54. Lewis, B. A., and Engelman, D. M. (1983) Lipid bilayer thickness varies linearly with acyl chain length in fluid phosphatidylcholine vesicles, *J. Mol. Biol. 166*, 211−217.
55. Marsh, D. (1990) *Handbook of Lipid Bilayers*, CRC, Boca Raton, FL.
56. Martinez-Senac Mdel, M., Corbalan-Garcia, S., and Gomez-Fernandez, J. C. (2002) The structure of the C-terminal domain of the pro-apoptotic protein Bak and its interaction with model membranes, *Biophys. J. 82*, 233−243.
57. Azpiazu, I., Gomez-Fernandez, J. C., and Chapman, D. (1993) Biophysical studies of the Pf1 coat protein in the filamentous phage, in detergent micelles, and in a membrane environment, *Biochemistry 32*, 10720−10726.
58. Martinez-Senac, M. D., Corbalan-Garcia, S., and Gomez-Fernandez, J. C. (2000) Study of the secondary structure of the C-terminal domain of the antiapoptotic protein Bcl-2 and its interaction with model membranes, *Biochemistry 39*, 7744−7752.
59. El Kirat, K., Lins, L., Brasseur, R., and Dufrene, Y. F. (2005) Fusogenic tilted peptides induce nanoscale holes in supported phosphatidylcholine bilayers, *Langmuir 21*, 3116−3121.
60. Lundberg, P., and Langel, U. (2003) A brief introduction to cell-penetrating peptides, *J. Mol. Recognit. 16*, 227−233.
61. Borchardt, K., Heber, D., Klingmuller, M., Mohr, K., and Muller, B. (1991) The Ability of Cationic Amphiphilic Compounds to Depress the Transition-Temperature of Dipalmitoylphosphatidic Acid Liposomes Depends on the Spatial Arrangement of the Lipophilic Moiety, *Biochem. Pharmacol. 42*, S61−S65.
62. Kursch, B., Lullmann, H., and Mohr, K. (1983) Influence of various cationic amphiphilic drugs on the phase-transition temperature of phosphatidylcholine liposomes, *Biochem. Pharmacol. 32*, 2589−2594.
63. Berquand, A., Mingeot-Leclercq, M. P., and Dufrene, Y. F. (2004) Real-time imaging of drug-membrane interactions by atomic force microscopy, *Biochim. Biophys. Acta 1664*, 198−205.
64. Berquant, A., Fa, N., Dufrene, Y. F., and Mingeot-Leclercq, M. P. (2005) Interaction of the macrolide antibiotic azithromycin with lipid bilayers: Effect on membrane organization, fludity, and permeability, *Pharm. Res. 22*, 465−475.
65. Ramstedt, B., and Slotte, J. P. (2002) Membrane properties of sphingomyelins, *FEBS Lett. 531*, 33−37.
66. Barenholz, Y., and Cevc, G. (2000) Structure and properties of membranes, in *Physical Chemistry of Biological Interfaces* (Baskin, A., Norde, W., Eds.) pp 171−241, Dekker: New York.
67. Janshoff, A., Bong, D. T., Steinem, C., Johnson, J. E., and Ghadiri, M. R. (1999) An animal virus-derived peptide switches membrane morphology: possible relevance to nodaviral transfection processes, *Biochemistry 38*, 5328−5336.
68. Simon, S. A., and McIntosh, T. J. (1984) Interdigitated hydrocarbon chain packing causes the biphasic transition behavior in lipid/alcohol suspensions, *Biochim. Biophys. Acta 773*, 169−172.
69. Kinoshita, K., and Yamazaki, M. (1996) Organic solvents induce interdigitated gel structures in multilamellar vesicles of dipalmitoylphosphatidylcholine, *Biochim. Biophys. Acta 1284*, 233−239.
70. Saalik, P., Elmquist, A., Hansen, M., Padari, K., Saar, K., Viht, K., Langel, U., and Pooga, M. (2004) Protein cargo delivery properties of cell-penetrating peptides. A comparative study, *Bioconjugate Chem. 15*, 1246−1253.
71. Seydel, J. K., and Wiese, M. (2002) *Drug-Membrane Interactions*, Wiley-VCH, Weinheim.
72. Matsuzaki, K., Fukui, M., Fujii, N., and Miyajima, K. (1993) Permeabilization and Morphological-Changes in Phosphatidylglycerol Bilayers Induced by an Antimicrobial Peptide, Tachyplesin-I, *Colloid Polym. Sci. 271*, 901−908.
73. Gidalevitz, D., Ishitsuka, Y., Muresan, A. S., Konovalov, O., Waring, A. J., Lehrer, R. I., and Lee, K. Y. (2003) Interaction of antimicrobial peptide protegrin with biomembranes, *Proc. Natl. Acad. Sci. U.S.A. 100*, 6302−6307.
74. Schibli, D. J., Epand, R. F., Vogel, H. J., and Epand, R. M. (2002) Tryptophan-rich antimicrobial peptides: comparative properties and membrane interactions, *Biochem. Cell Biol. 80*, 667−77.

BI050923C